GEOPHYSICAL RESEARCH LETTERS

Supporting Information for ”A toy model to investigate stability of AI-based dynamical systems”

B. Balogh[1], D. Saint-Martin[1], A. Ribes[1]

[1]CNRM, Université de Toulouse, Météo-France, CNRS, Toulouse, France

Contents of this file

1. Text S1
2. Figures S1 to S3

Corresponding author: Blanka Balogh, CNRM, Université de Toulouse, Météo-France, CNRS, Toulouse, France. (blanka.balogh@meteo.fr)

Introduction

In this Supporting Information, we investigate the stability issues with a simpler model than the eL63 toy model described in the main text. The use of this simple model supports the results obtained in the main text. The state vector of this simple dynamical system belongs to $\mathbb{R}^3$, allowing a simple graphical representation and thus facilitating interpretation of stability issues discussed in the main text. Text S1 describes the simpler model and additional figures (Figures S1-S3) provide more information about the stability issues encountered by neural networks.

Text S1.

The numerical instability issue is investigated by using a very simple model. Instead of the Lorenz'63 model we assume a rotation along a circular path. As the embedded L63 model, the model is defined in two steps.

In a first step, we define the time evolution of the state vector $\mathbf{z} = (z_1, z_2, z_3) \in \mathbb{R}^3$ by :

$$\begin{aligned} \dot{z}_1 &= -\omega z_2, \\ \dot{z}_2 &= \omega z_1, \\ \dot{z}_3 &= -\kappa z_3. \end{aligned} \tag{1}$$

The first two equations describe a simple rotation along a circle of radius R (we will set $R = 1$) with a constant rotational speed, $\omega = \frac{2\pi}{T} = \dot{\theta}$. T is the rotation period and $(z_1(t), z_2(t)) = (\cos\theta(t), \sin\theta(t))$, with $\theta(t) = \omega t$. The third additional equation is a simple restoring force (we fix $\kappa = 1$).

In a second step, we apply a random rotation (consistent with eL63) to derive the state vector of the system, $\mathbf{x} = (x_1, x_2, ..., x_d)$:

$$\mathbf{x}(t) = P\mathbf{z}(t), \tag{2}$$

where $P \in \mathbb{R}^{3\times 3}$ is the rotation matrix (P does not depend on time).

This system of equations can be formally rewritten $\dot{\mathbf{x}}(t) = f(\mathbf{x}(t))$. To replace the 'true' function f, we fit an approximate function with neural networks trained on a single orbit of the dynamical model, $\widehat{f_{orb}}$. We choose $T = 100$; the learning orbit is obtained by integrating Eqs. (1) and (2) with a time-step of $\Delta t = 1$. The numerical integration is performed over 5 periods, corresponding to 500 model time units (MTU, where 1 MTU $= 1\ \Delta t$).

Figure S1 compares the value of f, $\widehat{f}_{orb}$ in the plane $\{-2 \leq z_1 \leq 2, -2 \leq z_2 \leq 2, z_3 = 0\}$ and over the cylinder $\{0 \leq \arctan(z_2/z_1) \leq 2\pi, -1 \leq z_3 \leq 1\}$. In the plane $z = 0$, errors are very small but no restoring force is learnt by $\widehat{f}_{orb}$ (as one might expect given the learning sample). So, as soon as the trajectory deviates from the $z = 0$ plane, errors can grow and bring the predicted state vector in out-of-sample regions, where prediction errors are larger. This is illustrated in Figures S2 and S3. Figure S2 shows the orbit of the dynamical system driven by a typical $\widehat{f}_{orb}$, from an initial condition : $\mathbf{z} = (1, 0, 0)$. The trajectory of $(z_1(t), z_2(t))$ is illustrated in Figure S2(a) and the time evolution of the third component $(z_3(t))$ is plotted in Figure S2(b). After about 2 periods of rotation ($t_1 = 1.5T$ $= 150$ MTUs), the trajectory remains relatively close to the true orbit, but $z_3(t_1) > 0$ and $z_3(t)$ is raising slowly. The vector fields in the corresponding $z_3 = z_3(t_1)$-plane are shown in Figure S3(a) and (d). In this plane, $(\dot{z}_1, \dot{z}_2)$ predicted by $\widehat{f}_{orb}$ are less accurate than in the initial (and learning) $z_3 = 0$ plane. As time goes on, the error on the z_3 component increases and the vector field $(\dot{z}_1, \dot{z}_2)$ no longer accurately reproduces the rotation along the circle. This leads to an orbit that deviates from the original circle and an exponential growth of error on the third component (see Figures S3(b), (c), (e) and (f)).

This remarkably simple model is a perfectly periodic and predictable system. Various statistical techniques could successfully forecast the state of this system at a given lead-time. However, learning the derivative of this system (as done in climate modeling) can cause stability issues.

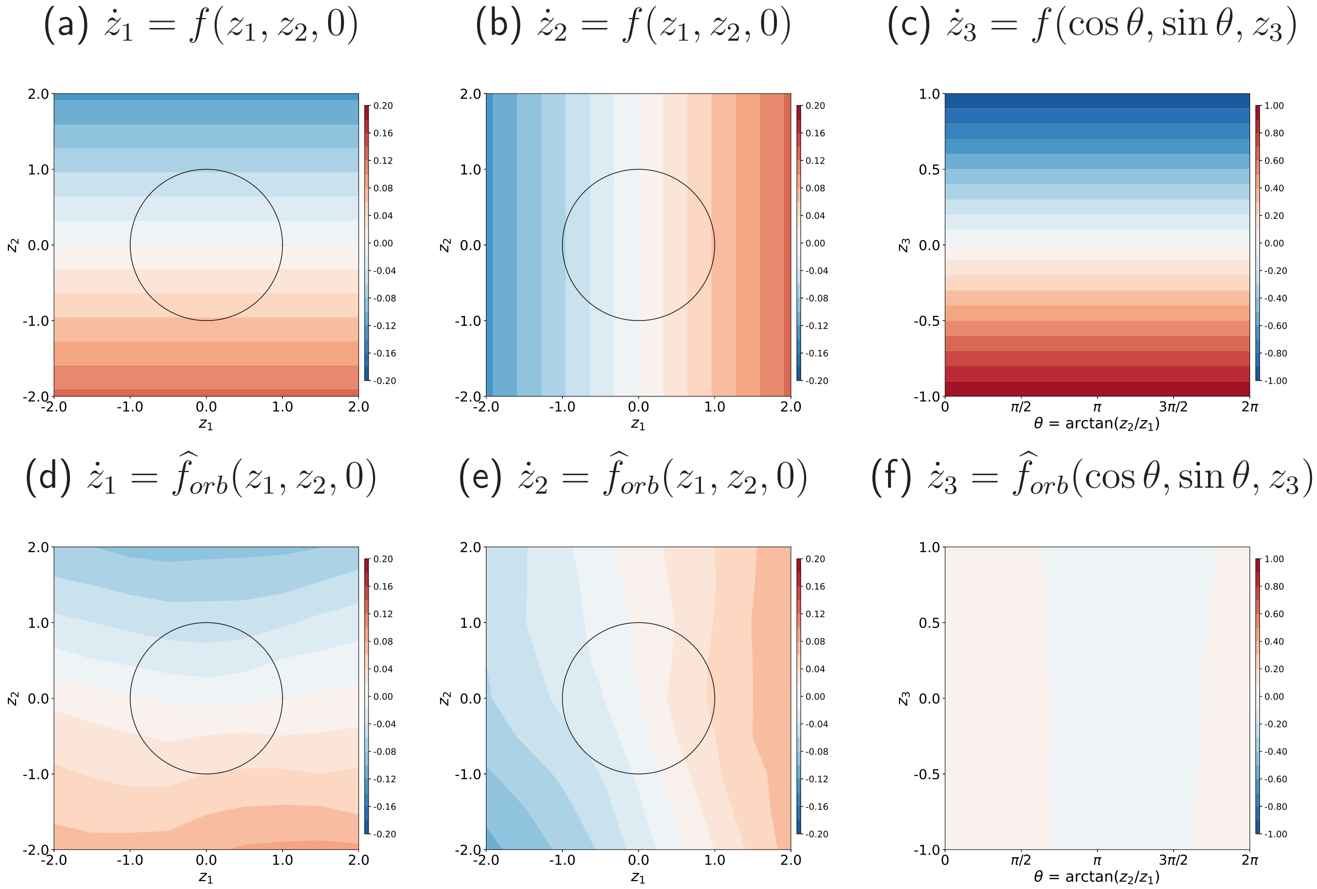

(a) $\dot{z}_1 = f(z_1, z_2, 0)$ (b) $\dot{z}_2 = f(z_1, z_2, 0)$ (c) $\dot{z}_3 = f(\cos\theta, \sin\theta, z_3)$

(d) $\dot{z}_1 = \widehat{f}_{orb}(z_1, z_2, 0)$ (e) $\dot{z}_2 = \widehat{f}_{orb}(z_1, z_2, 0)$ (f) $\dot{z}_3 = \widehat{f}_{orb}(\cos\theta, \sin\theta, z_3)$

Figure S1. Values of $\dot{z}_1$, $\dot{z}_2$ and $\dot{z}_3$ obtained with f (top) and $\widehat{f}_{orb}$ (bottom). The values of $\dot{\mathbf{z}}$ are computed in the plane $\{-2 \leq z_1 \leq 2, -2 \leq z_2 \leq 2, z_3 = 0\}$ on panels (a), (b), (d) and (e), and over the cylinder $\{0 \leq \theta = \arctan(z_2/z_1) \leq 2\pi, -1 \leq z_3 \leq 1\}$ on panels (c) and (f).

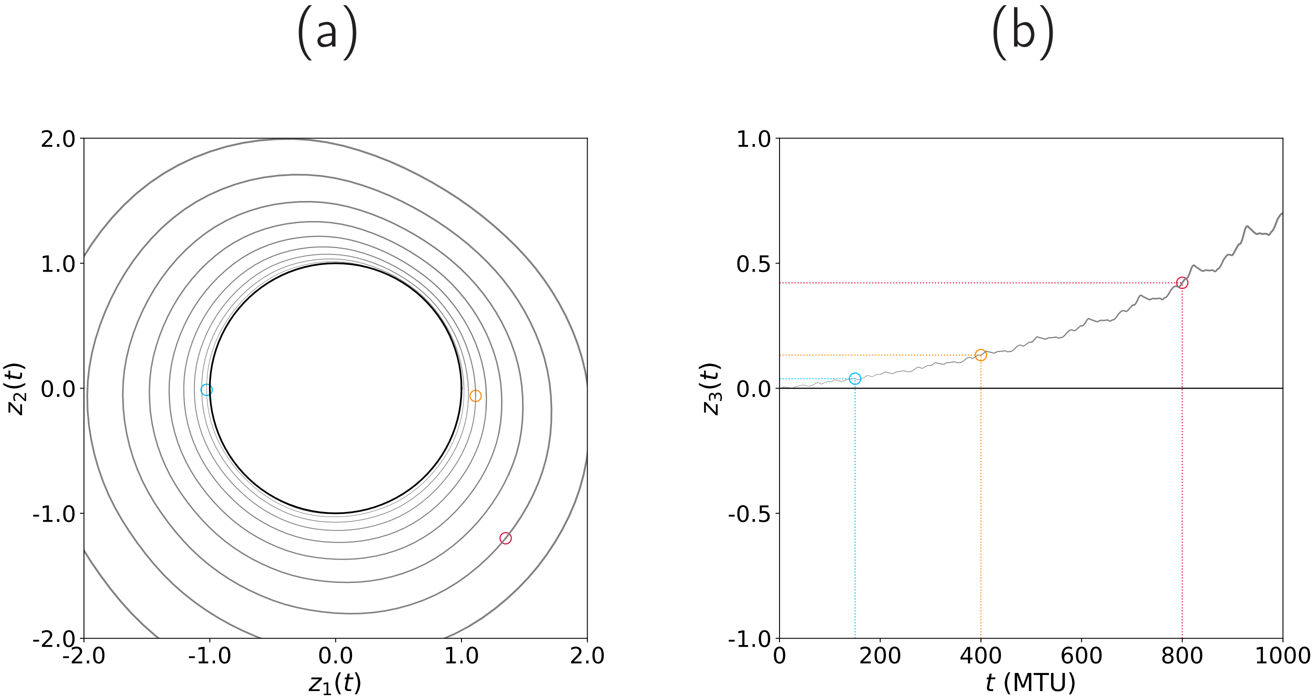

Figure S2. Temporal evolution of (a) the state vector $(z_1(t), z_2(t))$ and (b) the third component $z_3(t)$ for an orbit driven by $\widehat{f}_{orb}$ (grey lines) and for the true orbit driven by f (black lines). The initial condition is $\mathbf{z} = (1, 0, 0)$ and the orbits are plotted for the first 1000 MTUs. The state of the vector $\mathbf{z}$ at $t = \{150, 400, 800\}$ is highlighted by a colored empty circle.

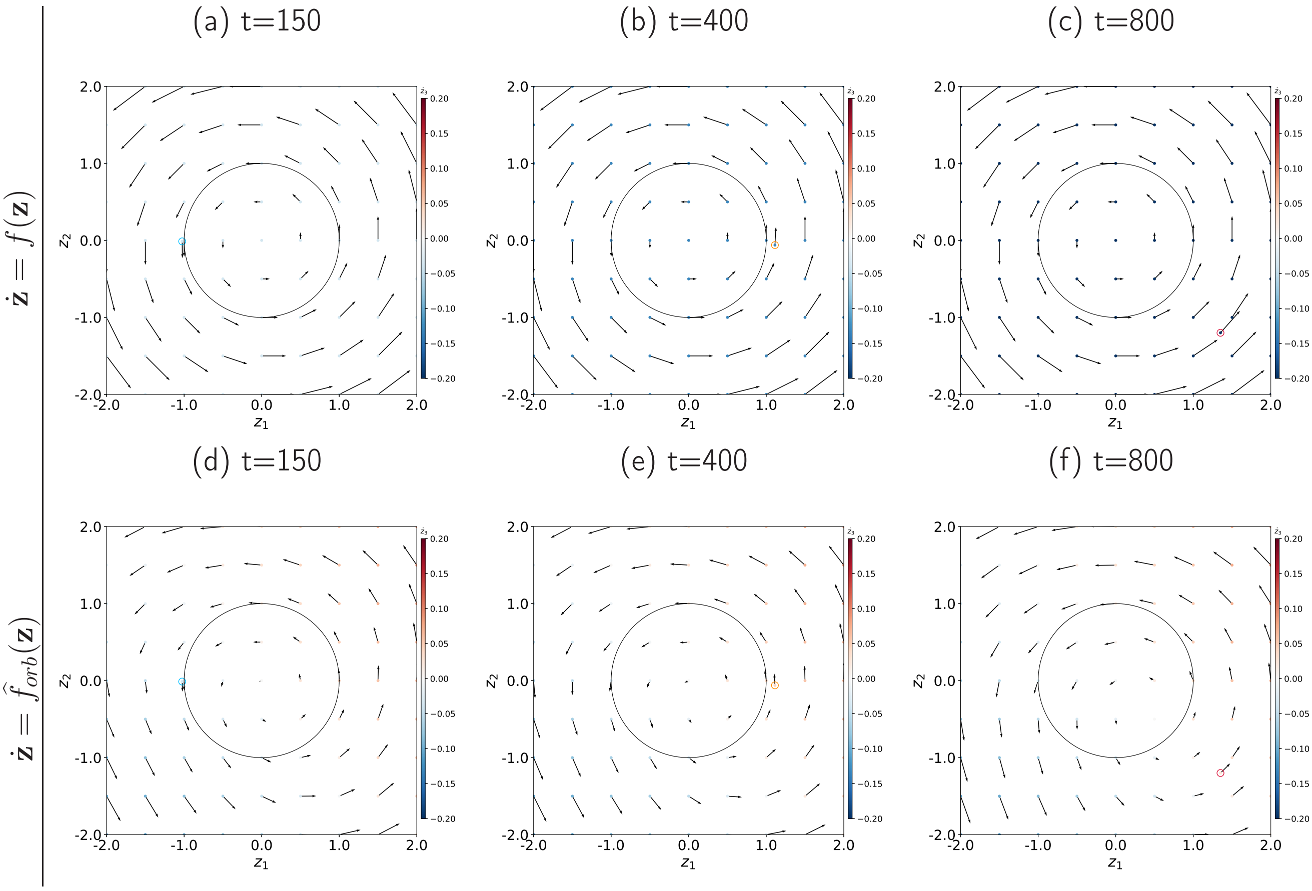

Figure S3. Snapshots at $t = \{150, 400, 800\}$ of the vector fields $\dot{\mathbf{z}}(t)$ predicted by f (top panels) and by $\widehat{f}_{orb}$ (bottom panels). $(\dot{z}_1, \dot{z}_2)$ are plotted using vectors and $\dot{z}_3$ is displayed by filled circles. The state of $(z_1(t), z_2(t))$ at $t = \{150, 400, 800\}$ is represented by a colored empty circle (same color convention as Figure S2).